

## Article

# Surface Chemistry of Cherry Stone-Derived Activated Carbon Prepared by H<sub>3</sub>PO<sub>4</sub> Activation

Jose M. González-Domínguez <sup>1,\*</sup>, Carmen Fernández-González <sup>2</sup>, María Alexandre-Franco <sup>2</sup>  
and Vicente Gómez-Serrano <sup>2,\*</sup>

<sup>1</sup> Carbon Nanostructures and Nanotechnology Group, Instituto de Carboquímica (ICB-CSIC), c/Miguel Luesma Castán 4, 50018 Zaragoza, Spain

<sup>2</sup> Department of Organic and Inorganic Chemistry, University of Extremadura, Avd. Elvas s/n, 06071 Badajoz, Spain; mcfernan@unex.es (C.F.-G.); malexandre@unex.es (M.A.-F.)

\* Correspondence: jmgonzalez@icb.csic.es (J.M.G.-D.); vgomez@unex.es (V.G.-S.)

**Abstract:** The preparation of activated carbons (ACs) from cherry stones and chemical activation with H<sub>3</sub>PO<sub>4</sub> can be controlled by the experimental variables during the impregnation step in order to obtain a tailored porous structure of the as-prepared ACs. This control not only extends to the ACs' texture and porosity development, but also to the chemical nature of their surface. The spectroscopic and elemental characterization of different series of ACs is presented in this study. The spectroscopic band features and assignments strongly depend on the H<sub>3</sub>PO<sub>4</sub> concentration and/or the semi-carbonization treatments applied to the feedstock before impregnation, which ultimately influence different characteristics such as the AC hydrophilicity. Different surface chemistries arise from the different tailored impregnation solutions, showing a practical outcome for future applications of the as-prepared ACs.

**Keywords:** biomass; activated carbon; chemical activation; phosphoric acid; surface chemistry



**Citation:** González-Domínguez, J.M.; Fernández-González, C.; Alexandre-Franco, M.; Gómez-Serrano, V. Surface Chemistry of Cherry Stone-Derived Activated Carbon Prepared by H<sub>3</sub>PO<sub>4</sub> Activation. *Processes* **2024**, *12*, 149. <https://doi.org/10.3390/pr12010149>

Academic Editor: Adrián Bogeat-Barroso

Received: 21 December 2023

Revised: 31 December 2023

Accepted: 5 January 2024

Published: 8 January 2024



**Copyright:** © 2024 by the authors. Licensee MDPI, Basel, Switzerland. This article is an open access article distributed under the terms and conditions of the Creative Commons Attribution (CC BY) license (<https://creativecommons.org/licenses/by/4.0/>).

## 1. Introduction

Activated carbon (AC) is a synthetic kind of carbon material characterized by a large surface area and porosity developments [1], and the presence on its surface of a variety of oxygen functional groups. These properties confer AC a high adsorption capacity and versatility, which make it a unique and nearly universal adsorbent of gases, vapors and solutes in solution. As a result, AC is used in a wide range of liquid- or gas-phase separation, purification, catalysis and pollution control processes [2]. The key factor for the performance of AC in such processes depends on the starting material and the method used in its preparation. On an industrial scale, this is usually accomplished using carefully chosen experimental parameters in order to obtain specific adsorbents from low-cost precursors with the minimum energy consumption. One suitable AC precursor is cherry stones (CSs, hereafter) [3–5], from which AC has been developed as usual by the two stages of physical and chemical activation methods. As far as the chemical method is concerned, ZnCl<sub>2</sub> [6,7], KOH [8,9] and H<sub>3</sub>PO<sub>4</sub> [10,11] have been used as activating agents for such a purpose. Of the aforesaid activating agents, H<sub>3</sub>PO<sub>4</sub> has been the most investigated and preferred, due to environmental and safety issues. It causes porosity development through acid-base bond cleavages and also through complex processes, such as cyclization and condensation, involving biopolymers that eventually form phosphorous bridges and the insertion of phosphate groups whose physical expansion leads to accessible pores [12]. These pores are paramount traits for the AC's eventual use in specific applications, for instance as supercapacitor electrodes. In this field, Yang et al. [13] proposed a new strategy for pore structure regulation together with heteroatom doping of ACs that significantly reduced the overall electrical resistance (by ~50%), thus improving the rate performance and power density.

In the process of AC preparation by  $\text{H}_3\text{PO}_4$  activation, the impregnation stage is crucial because of the trend of  $\text{H}_3\text{PO}_4$  in aqueous solution to become molecularly self-associated, with consequent size and viscosity increases, which must decisively influence the degree of  $\text{H}_3\text{PO}_4$  diffusion in the bulk of precursor mass and, as a final result, the activating action of  $\text{H}_3\text{PO}_4$ . In fact, from the results obtained in previous studies it became apparent that the impregnation of CSs with  $\text{H}_3\text{PO}_4$  only affected in part the mass bulk of the material, whereas a significant portion remained phosphorus-free after the impregnation treatment [14–17]. During the subsequent carbonization/activation stage at a high temperature in a  $\text{N}_2$  atmosphere, the resulting product would locally suffer either activation or simply pyrolysis to an extent depending on the degree of previous impregnation of the CSs with  $\text{H}_3\text{PO}_4$ . Needless to say, a partial impregnation of the CSs would mitigate the process of  $\text{H}_3\text{PO}_4$  activation in terms of porosity development and effectiveness. As a guide, it appears likely that a reduced diffusion and thereby concentration  $\text{H}_3\text{PO}_4$  in the AC precursor would promote the development of large porosity to the detriment of narrow porosity.

In earlier studies, with a view to controlling the diffusion of  $\text{H}_3\text{PO}_4$  in CSs, the impregnation of CSs with  $\text{H}_3\text{PO}_4$  was carried out using acid solutions of varying concentration, aliquot parts of a given  $\text{H}_3\text{PO}_4$  solution, a residual solution of  $\text{H}_3\text{PO}_4$  after impregnation and so on [15]. Likewise, previously heat-treated  $\text{H}_3\text{PO}_4$  solutions and CSs were used in the impregnation treatment with  $\text{H}_3\text{PO}_4$ . The obtained results showed that the impregnation method significantly influenced mass balances and textural changes [15–17]. The alteration of the biopolymers structure in the feedstock before impregnation could be another way to control their interaction with  $\text{H}_3\text{PO}_4$ . The lignocellulosic material can be altered by thermal treatments (semi-carbonizations) that partially volatilize and modify the constituent biopolymers [16,18]. The acid concentration, impregnation procedure and other experimental issues can be chosen to obtain a controlled development of porosity, enabling its tailoring to satisfy the requirements of a particular application [16]. Nevertheless, an open question still arises as to how the actuation of experimental variables (for the production of ACs from CSs using  $\text{H}_3\text{PO}_4$  as the activating agent) affects the surface chemistry of such ACs.

The surface chemistry of ACs plays an important role in their adsorption performance against different adsorbates [19]. Some modification methodologies, using either physical or chemical treatments, allow the obtaining of materials with specific surface properties, so it is possible to adapt the ACs in this way to different needs, thus developing greater selectivity against targeted adsorbates [20]. Surface modifications are mainly carried out by oxidizing the surface in post-synthesis stages, which tend to produce a hydrophilic structure with a large number of oxygen-containing groups. The concentration of functional groups can be reduced by heat treatment in an inert atmosphere at established temperature ranges. This is because the stability of the functional groups found on the surface of an AC displays a unique decomposition scheme [14], revealing a varied and rich surface chemistry, so, by combining these two methods (chemical oxidation and thermal decomposition), a desired oxidation degree may be achieved. This allows in turn the study of the interactions of different functional groups with adsorbates such as metallic ions [21]. However, there is a visible lack as to taking advantage of the native AC surface chemistry, particularly when the chemical activation procedure of the feedstock is modified with a view to tailoring the eventual AC porous structure. Acquiring insights into the tuning of the surface composition from the initial synthesis stages would enable a complete tailoring of the ACs physicochemical characteristics avoiding subsequent oxidation or thermal steps.

In this present work, ACs prepared by chemical activation of CSs (with or without previous semi-carbonization) using  $\text{H}_3\text{PO}_4$  as the activating agent are revisited from previous studies [15–17]. For a full characterization of their porous structure and preparation yields, we refer the reader to such previous works. These ACs are herein characterized by elemental analyses and different spectroscopic techniques in order to elucidate the influence of the methodological variations of chemical activation on their eventual surface chemistry, which is deemed to be closely tied to the preparation procedure.

## 2. Materials and Methods

### 2.1. Feedstock and Activated Carbon Preparation

CSs from Valle del Jerte (province of Cáceres, Spain) were used as the precursor. CSs were milled and sieved until the particle size was between 1 and 2 mm. This granulated precursor was washed by soaking overnight in diluted aqueous sulfuric acid (5% *v/v*), thoroughly rinsed with distilled water (until pH neutral) and then dried for 24 h in an oven at 120 °C.

In a typical impregnation experiment, 25 g of CSs were soaked in a beaker with 100 mL of various H<sub>3</sub>PO<sub>4</sub> aqueous solutions at 85 °C for 2 h, under constant magnetic stirring. In order to prevent solvent losses, the beaker was sealed with a latex film during the entire impregnation process [15]. The resulting impregnated material was oven-dried overnight at 120 °C and stored in desiccator for further carbonization. The impregnated materials were carbonized in a cylindrical horizontal furnace. An amount of 8 g of impregnated material was placed into a ceramic crucible and treated at 500 °C for 2 h under a nitrogen atmosphere (100 mL/min flow). The isothermal stage was reached at a 10 °C/min heating rate. The choice of the carbonization temperature was based on previous studies which determined 500 °C to be the optimal temperature, as it maximizes the surface area obtained by the BET method [14]. The ACs were washed in Soxhlet equipment with distilled water for two days in order to remove the remaining traces of H<sub>3</sub>PO<sub>4</sub>. These removable traces are phosphorus species weakly bonded to the carbonaceous backbone of the ACs and can be thus lixiviated. The eventual AC samples receive the same name as their impregnated predecessors but ending in A, standing for activated. The samples were finally oven-dried at 120 °C for 12 h. A graphical scheme (Figure S1) displaying the full set of samples is shown in Supplementary Materials.

A series of samples (Series 1, Table 1) was prepared by the impregnation of CSs with diluted H<sub>3</sub>PO<sub>4</sub> aqueous solutions [16,17]. The samples D and DI1 were impregnated with diluted solutions containing 16 g H<sub>3</sub>PO<sub>4</sub>/100 mL and 10.66 g H<sub>3</sub>PO<sub>4</sub>/100 mL, respectively. The samples DL1, DL2 and DL3 were impregnated once, twice and three times, respectively, with a solution of 5.33 g H<sub>3</sub>PO<sub>4</sub>/100 mL. It should be noted that the total amounts of phosphoric acid put in contact with the CSs were identical for the samples D and DL3, and also for the samples DI1 and DL2, respectively. Samples DF and DFW were impregnated in the same way as sample D, but DF was filtered in a glass filter, and DFW was filtered and rinsed with water, before drying them overnight at 120 °C. The sample DRL was impregnated with the filtered residual liquid obtained during the preparation of DF. This residual liquid is a diluted H<sub>3</sub>PO<sub>4</sub> solution containing semi-impregnated lignocellulosic particles and other organic products.

**Table 1.** Elemental, immediate analysis and XPS-derived surface atomic composition for all the AC samples studied.

Samples	Elemental Analysis (wt%)				Moisture (wt%)	Ashes (wt%)	Surface at. %			
	C	H	N	O + P			C	N	O	P
<b>Series 1</b>										
DA	75.4	2.1	0.42	22.1	7.3	2.5	80.5	2.0	15.2	2.0
DL1A	74.1	2.1	0.38	23.5	4.9	2.5	84.9	1.4	11.4	2.3
DL2A	75.1	2.3	0.42	22.2	7.4	2.3	86.1	0.5	10.9	2.5
DI1A	70.9	2.3	0.38	26.4	10.9	1.9	82.3	1.1	13.9	2.8
DL3A	61.4	3.1	0.36	35.1	23.2	2.6	82.6	1.7	13.1	2.6
DFA	73.4	2.1	0.33	24.2	5.5	1.8	84.5	1.5	11.9	2.2
DFWA	86.6	2.5	0.47	10.4	2.5	1.9	87.3	2.3	10.4	~0
DRLA	74.6	2.1	0.40	22.9	7.1	1.5	82.8	1.9	12.9	2.3
<b>Series 2</b>										
C0A	59.9	1.2	0.15	38.7	8.7	3.1	91.2	~0	6.7	2.1
C2A	67.6	1.8	0.14	30.5	8.6	3.4	88.2	~0	8.8	2.9
C6A	69.0	1.7	0.30	29.0	11.6	3.7	90.1	~0	7.6	2.3
C12A	68.5	1.6	0.17	29.8	6.1	3.9	90.8	~0	7.0	2.2
C24A	64.9	2.1	0.17	32.9	15.4	4.0	87.3	~0	9.8	2.9
<b>Series 3</b>										
S200DA	74.1	2.6	0.36	23.3	7.7	2.3	85.8	~0	11.6	2.6
S300DA	69.9	2.4	0.46	27.3	6.6	3.2	82.7	1.2	12.4	2.9
S200CA	54.7	1.2	0.18	44.0	5.2	3.6	85.7	~0	10.8	3.5
S300CA	66.5	2.7	0.44	30.5	11.1	5.1	75.1	0.9	17.7	2.9

Another series of samples (Series 2, Table 1) was made by impregnating CSs with concentrated solutions of  $\text{H}_3\text{PO}_4$ . As-purchased phosphoric acid (PANREAC 85%, 1.7 g/mL) was directly utilized for the preparation of sample C0. The  $\text{H}_3\text{PO}_4$  concentration in this impregnation (144.5 g  $\text{H}_3\text{PO}_4$ /100 mL) was approximately nine times the concentration used for sample D (Series 1, 16g  $\text{H}_3\text{PO}_4$ /100 mL). For the preparation of samples C2, C6, C12 and C24, commercial phosphoric acid was over-concentrated by heating in an oven at 120 °C for 2, 4, 6, 12 and 24 h, respectively. Over-concentrated  $\text{H}_3\text{PO}_4$  solutions were put in contact with CSs immediately after their preparation.

Four samples (Series 3, Table 1) were prepared to study the effect of semi-carbonization processes before the impregnation with  $\text{H}_3\text{PO}_4$ . CSs were treated in a vertical cylindrical furnace at 200 °C or 300 °C for 2 h under a nitrogen atmosphere (100 mL/min flow, 10 °C/min heating ramp) to obtain the semi-carbonized products (S200 and S300, respectively). Both S200 and S300 were impregnated with a diluted  $\text{H}_3\text{PO}_4$  solution of 16 g/100 mL (samples S200D and S300D), and with a concentrated solution of 144.5 g  $\text{H}_3\text{PO}_4$ /100 mL (samples S200C and S300C). The impregnation procedures for samples D, S200D and S300D are identical, but the precursors are CSs, S200 and S300, respectively. Also, the impregnation procedures for samples C0, S200C and S300C are identical but the precursors are different.

## 2.2. Characterization Techniques

Immediate analyses (moisture and ash content) were performed by subjecting the AC samples to controlled heating and weighing. In a Thermo Electron-Heraeus (Asheville, NC, USA) oven at 150 °C with forced ventilation in an inert atmosphere, the moisture content was ascertained by successive periods of heating (1 h) and weighing compared to the initial weight. The final number was collected after three consecutive identical weight readings, in which moisture corresponded to the proportional % weight loss with respect to the initial AC weight. The ashes content was obtained by heating in a muffle furnace, CRN-48 from Hobersal (Barcelona, Spain), with a working range up to 1250 °C. The remaining solid residue after fully burning the sample was taken as the ash content in comparison to the initial AC weight.

Elemental analyses (as regards to C, H, N and S wt%) were performed in a Carlo Erba (Barcelona, Spain) Thermo Flash 1112 device using oven-dried and thoroughly milled samples. For a typical C, H, N and S determination, samples are burnt in pure oxygen at 950 °C in the presence of  $\text{V}_2\text{O}_5$ . Combustion products pass through an oxidant bed of CuO at 950 °C to be converted into  $\text{NO}_x$ ,  $\text{CO}_2$  and  $\text{H}_2\text{O}$ . Then, a reductor bed of metallic Cu at 500 °C transforms  $\text{NO}_x$  into  $\text{N}_2$ . The gases are separated in a polar chromatographic column and quantified by thermal conductivity.

Infrared (IR) spectra were obtained using Thermo Electron Corp (Waltham, MA, USA). IR-300 equipment. Identical amounts (0.5 mg) of the AC sampled were milled in an agate mortar and mixed with 230 mg of spectroscopic-grade KBr. The powder mixtures were pressed at 10 Tons for 3 min to obtain pellets for IR measurements.

X-ray photoelectron spectroscopy (XPS) measurements were carried out using K-Alpha Thermo Scientific (Waltham, MA, USA) equipment under high vacuum conditions ( $2 \times 10^{-7}$  mbar). A monochromatic radiation of 1486.68 eV (Al  $K\alpha$  line) was used to irradiate samples perpendicularly at 12 kV. Additionally, a flood gun device (working at 4.2 mA) compensated for the load losses. The register settings were established as 50 ms accumulation time for each step in all cases. Survey spectra were recorded by 1 eV energy steps and 20 scans, while 0.1 eV steps were taken for specific regions (30 scans in  $\text{C}_{1s}$  and 40 scans in  $\text{O}_{1s}$  and  $\text{P}_{2p}$ ). The obtained spectra were calibrated in the  $\text{C}_{1s}$  region by taking the C-C contribution as 284.4 eV [22]. The numerical treatment was performed with the XPSpeak 4.1 software tool, and the background corrections effected with Shirley functions. The deconvoluted spectra for each specific region ( $\text{C}_{1s}$ ,  $\text{O}_{1s}$  and  $\text{P}_{2p}$ ) were obtained after imposing several constraints, in order to maximize the quality of the fitting. These constraints were mainly those concerning the peak full width at half maximum (FWHM), which was restricted to the 1.3–2.5 eV range, and the Gaussian-to-Lorentzian

ratio, which was forced to be in the range of 75–90% in C1s contributions, except for the C-C band at ~284.4 eV. Asymmetry corrections were not applied.

### 3. Results and Discussion

#### 3.1. Chemical Analyses

Elemental and immediate analyses for the different prepared samples are shown in Table 1. It is worth mentioning that the obtained wt% in sulphur was zero for all AC samples and, therefore, the difference between C, H and N can be reasonably ascribed to the oxygen and phosphorus content. This joint content is higher in Series 2 than for the first one. Oxygen may be part of the AC structure also as phosphate or phosphonate groups.

The moisture of the ACs is affected by their hydrophilic character, porous structure and surface development. Moisture data in Table 1 show that the impregnation with diluted  $H_3PO_4$  (samples with “D” in their code name) provides ACs with higher hydrophilicity when more  $H_3PO_4$  is retained in the feedstock (i.e., with higher  $H_3PO_4$  concentrations, higher number of impregnations or in the absence of filtration or washing of the impregnated CSs). In Series 2, large moisture contents are observed, with no clear order in the overconcentration time. The semi-carbonization process seems to enhance the hydrophilicity of the resulting ACs for samples impregnated with concentrated  $H_3PO_4$  (those with “C” in their code name). The ashes content is noticeably influenced by the retained amount of  $H_3PO_4$  in the samples, which experience mineralization at high temperatures. Ashes contents are higher for the second series of samples compared to the first one. A remarkable fact is the low overall ashes values observed, ranging from 1.5 wt% to 5.1 wt%. CSs are extremely suitable AC precursors, particularly for their intrinsically low inorganic components content [23]. A high inorganic fraction content may be lixiviated and be harmful for the AC’s further applications, such as as an electrolyte adsorbent in aqueous solution [24].

Oxygen + phosphorus contents follow a similar trend as observed for moisture. Higher  $H_3PO_4$  concentrations and/or semi-carbonization treatments lead to higher O + P percentages, most likely related to their moisture content and the formation of phosphate groups in the resulting ACs. Thus, these groups would be directly responsible for the hydrophilicity character in the studied samples. As regards Series 3 of the samples, these display the same outcomes as their AC analogues with non-treated CSs, showing that the previous semi-carbonization would not have a major impact on the eventual AC elemental composition, contrary to the AC porous structure [16,17] and preparation yields [15], as reported elsewhere.

#### 3.2. Surface Chemistry

IR spectroscopy is one of the most widely used experimental techniques for the study of surface functional groups in carbon materials. It has been extensively applied to the characterization of  $H_3PO_4$ -activated CSs [25]. Fourier transformed infrared (FTIR) spectra for Series 1, 2 and 3 samples are shown in Figure 1. In Series 1 of the samples there is a common band at  $\sim 1680\text{ cm}^{-1}$  for all samples, ascribable to the C=O bond stretching vibration. At around  $1100\text{ cm}^{-1}$  there is another common band, due to C-O bond stretching vibration. Similarly, the aromatic backbone bands can be observed at  $\sim 800\text{ cm}^{-1}$  and also at  $\sim 1000\text{ cm}^{-1}$  and  $\sim 1600\text{ cm}^{-1}$  (embedded in the previous bands). In Series 2 of the samples, a better general spectra resolution is observed. This is consistent with the elemental analysis data, where oxygen content was visibly higher in these samples. Carbonyl and ether bands can be again observed. The aromatic bands are better defined here, including also a prominent band at  $\sim 650\text{ cm}^{-1}$ . In Series 3 of the samples not only the effect of impregnating agent concentration is noticeable, but also the semi-carbonization treatment. For the S200 samples, the semi-carbonization effect is almost imperceptible, while, for the S300 samples, a highly oxidized surface is noticed from the spectra. Phenol and carboxylic groups are detected in regard to the bands at around  $1400$  and  $3200\text{ cm}^{-1}$  together with the previously reported bands. In these samples a very clear separation occurs between the aromatic and

the ether or carbonyl bands, with the first ones at about 900 (C=C stretching) and 1600  $\text{cm}^{-1}$  (C-H out-of-plane bending).

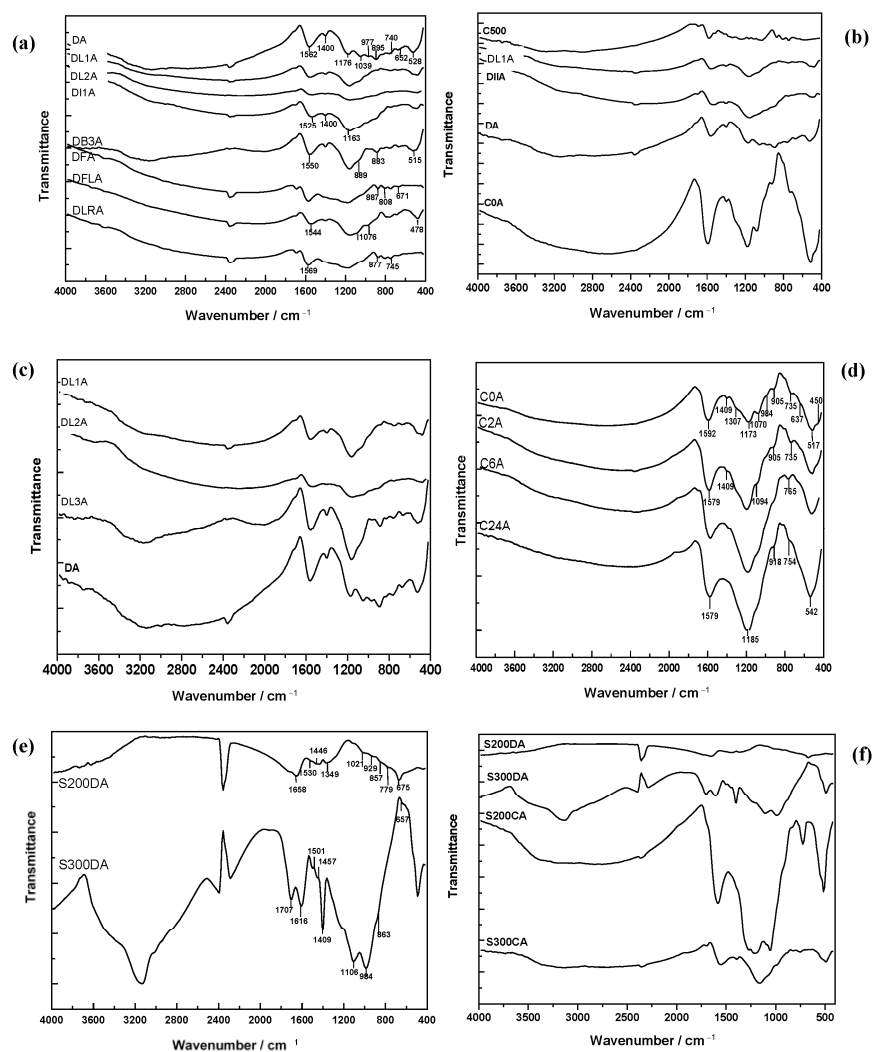


**Figure 1.** FTIR spectra for the different series of samples, grouped by: (a) impregnation with diluted phosphoric acid; (b) single impregnation procedure; (c) multiple impregnation procedure; (d) impregnation with concentrated phosphoric acid; (e) impregnation with diluted phosphoric acid (semi-carbonized feedstock); (f) impregnation with either diluted or concentrated phosphoric acid (semi-carbonized feedstock).

Interpretation of FTIR spectra is very often problematic due to the bands overlapping or the existence of alternative assignments. The previous assignments were made by attending to the existence of oxygenated groups on the AC surface. This determination is justified on the basis of the unequivocal presence of these groups in most similar carbonaceous materials, in particular those involving chemical interaction with inorganic acids. In this present work, not only oxygenated groups but also phosphorus ones are expected to appear in the FTIR spectra. Some possible vibrations can correspond to P=O stretching in phosphate (or polyphosphate) groups at around 1300  $\text{cm}^{-1}$  [26], C-O stretching in P-O-C(aromatic) groups (1163  $\text{cm}^{-1}$ ) and P-O-P stretching in polyphosphate chains (1065  $\text{cm}^{-1}$ ) [27]. In most of the samples, a very intense and broad band appears between 1173 and 1185  $\text{cm}^{-1}$  (with an elbow at 1070–1094  $\text{cm}^{-1}$ ), which is more intense in the samples of the second series. In some samples from Series 1, this band is hardly perceptible (i.e., the DL2A or DRLA samples). These results indicate an uneven presence of phosphorus groups among the series of samples. AC samples that exhibited the most remarkable

differences from the rest were the ones derived from the S300 semi-carbonized feedstock, where the enormous band at  $3200\text{ cm}^{-1}$  and bands at 1707, 1616, 1409, 1106 and  $984\text{ cm}^{-1}$  evidence their unique chemical surface nature with respect to the rest. The reason behind this fact is most likely to be related also to the difference exhibited in porous structure between S200- and S300-derived ACs. As we postulated in our previous work [16], the  $300\text{ }^{\circ}\text{C}$  semi-carbonization temperature, unlike that of  $200\text{ }^{\circ}\text{C}$ , originates changes in the cherry stones' original composition that affect the swelling and wetting behavior of  $\text{H}_3\text{PO}_4$  upon impregnation by partial de-volatilization of chemical species and the creation of an incipient porosity. Presumably, only small  $\text{H}_3\text{PO}_4$ -based species could then enter the pores while impregnating, thus generating a different surface functional groups distribution after activation.

The chemical composition of AC surfaces was further assessed by XPS analysis. From the survey spectra, registered in the binding energy range between 0 and 1350 eV, the identified peaks revealed that the main chemical composition of the ACs at the surface was mainly due to C, O and P, together with variable amounts of N which can be considered negligible in many cases. The atomic percentage composition at the surface was estimated through the relative areas under their corresponding peaks, and these data are presented in Table 1. The observed oxygen surface composition in Series 1 and 3 (~10–17 at.%) resemble that of commercial ACs oxidized by liquid-phase treatments, while the oxygen composition in Series 2 (~7–10 at.%) is more similar to that of commercial ACs oxidized by gas-phase treatments [28]. A significant difference between samples with different impregnation procedures can be noticed again. In Series 1 samples, the O/P ratio ranges around 4.5–7.5, indicating a noticeable presence of phosphate groups but also other oxygen-based functional groups (i.e., hydroxyl or ether, as determined by FTIR). The only exception to this series of samples is DFWA, which did not exhibit appreciable amounts of P in its surface. This clearly evidences the influence of the impregnation protocol, since in this case the CSs were filtered and washed before carbonization. This would have massively removed the retained phosphoric acid into the feedstock and thus the obtained AC exhibits mainly oxygen surface groups. The Series 2 samples show a substantially different trend, as the O/P ratio (~3) is approximately half of that in the former series, and there is no appreciable presence of nitrogen at the surface. The lower O/P ratio in the second series suggests that the chemical nature of the surface groups is different, pointing to the presence of P=O groups along with phosphates. With respect to the Series 3 samples, there is no clear trend of surface atomic composition regarding the impregnating  $\text{H}_3\text{PO}_4$  concentration, but there seems to be an influence of the semi-carbonization temperature.

The in-depth observation of specific regions within the XPS spectra corresponding to C, O and P elements allowed the obtaining of deeper insights into the surface chemistry of AC samples. Figure 2 gathers the main representative examples of the surface chemistry of ACs within the different series of samples (for a complete depiction of all the XPS spectra in specific regions, together with their peak parameters, see Supplementary Material). Table 2 collects the main information drawn from these spectra. For many authors, the C1s region is the most reliable in the characterization of ACs, but in our case the O1s and P2p regions also provided useful information regardless of their lower resolution. For all samples, the observation of the C1s core level showed that there is no evidence of the presence of carbides in any sample. Carbide carbons should appear at about 283 eV [29]. In contrast, the ACs backbone structures are mainly made of graphitic C-C bonds, as in all cases this is the primary contribution to the overall region; in addition, the  $\pi$ - $\pi^*$  shake-up contribution appearing at ~291 eV is typical of delocalized  $\text{sp}^2$  carbon structures. The  $\pi$  electron system of the basal planes in ACs is known to contribute to the carbon basicity [30]. The presence of surface oxygen groups can be denoted in C1s spectra through different contributions, as listed in Table 2. In general terms, there is a predominant presence of single C-O bonds in comparison to C=O bonds, but their ratio strongly depends on the impregnation procedure. For the DA sample (Figure 2a), the relative area (equivalent to the relative abundance) of C=O bonds and O-C=O bonds (belonging to carboxylic-

based groups) is very similar, together with a higher C-O contribution, suggesting that the oxygen-related surface chemistry of ACs impregnated with diluted  $H_3PO_4$  solutions is mainly due to hydroxyls and ethers, in good agreement with the FTIR spectra. The systematic dilution of the impregnation solution (example in DL3A sample, Figure 2b) provides even lower carboxylic content, as observed from the diminution of the O-C=O band, but an increase in the C=O band, possibly due to the progressive formation of acid anhydrides [30]. The semi-carbonization treatments, especially at 300 °C, clearly favors the contribution of O-C=O bonds with a visible decrease in the C=O band of the corresponding ACs (example in S300DA sample, Figure 2c), regardless of the impregnating  $H_3PO_4$  concentration. This would agree with the preferential appearance of carbonyl-containing functional groups, suggesting that carboxylic acids would predominate against phenols. The O1s spectra contributed to elucidate the chemical nature of the AC samples. The band contributions in this region are mostly due to single- and double-bonded oxygen atoms to carbon or phosphorus, centered at ~531.0 (double bonds) and ~532.7 (single bonds) eV, respectively. There is also a smaller contribution at around 535 eV which corresponds to chemisorbed oxygen or water [29]. The O1s contributions in the Series 1 samples generally show low presence of carboxylic and carbonyl-based groups, since a higher abundance of single-bonded oxygen in comparison to double-bonded (double-to-single ratio ~1/3) is found, which is consistent with the corresponding band ratios in the FTIR spectra of these samples. There is also agreement in the low chemisorbed water found for this series of samples (example in DL1A sample, Figure 2d), as the moisture content pointed to the lower hydrophilicity of samples impregnated with diluted  $H_3PO_4$  solutions compared to the concentrated ones. The filtering and washing of the impregnated feedstock before AC generation (sample DFWA, Figure 2e) provides a noticeable increase in the double-to-single oxygen bonds ratio (reaching a value that approaches to 1), which would be related to the impregnation procedure. For samples belonging to Series 2, a larger contribution of chemisorbed water is denoted, in consonance with the higher hydrophilicity of these AC samples. In addition, the double-bonded oxygen contribution experiences a slight downshift in binding energy (example in C2A sample, Figure 2f), indicating that there is a change in the chemical nature of these oxygen groups. This could be explained by the dramatic increase in phosphorus-based surface groups (such as phosphate), which possess many O=P bonds, upon the impregnation with concentrated  $H_3PO_4$ . Finally, the observation of the P2p region in the different AC samples allowed the identification of the phosphorus species located at the surface.

**Table 2.** Summary data obtained from the deconvolution of specific regions in XPS spectra.

Specific Region	Contributions			
	Range of Appearance (eV)	Area Range	Assignment	
C1s	284.3–284.6	47,000–79,000	C-C (graphitic)	
	285.8–286.2	9000–27,000	C-O	
	286.9–287.3	3000–10,000	C=O	
	288.6–289.3	4000–8000	O-C=O	
	290.8–291.1	1000–6000	$\pi$ - $\pi^*$	
O1s	530.6–531.3	5000–35,000	O=C/O=P	
	532.6–533.0	9000–42,000	O-C/O-P	
	534.7–536.4	500–6500	Chemisorbed O/H <sub>2</sub> O	
P2p	P2p 3/2	132.7–133.2	200–3500	$PO_4^{3-}$ and lineal polyphosphates
	P2p 1/2	133.7–134.5	0–2700	Cyclic phosphates (metaphosphates)
	P2p 3/2	137.0–137.5	0–500	Phosphine oxide (O=P-R <sub>3</sub> )

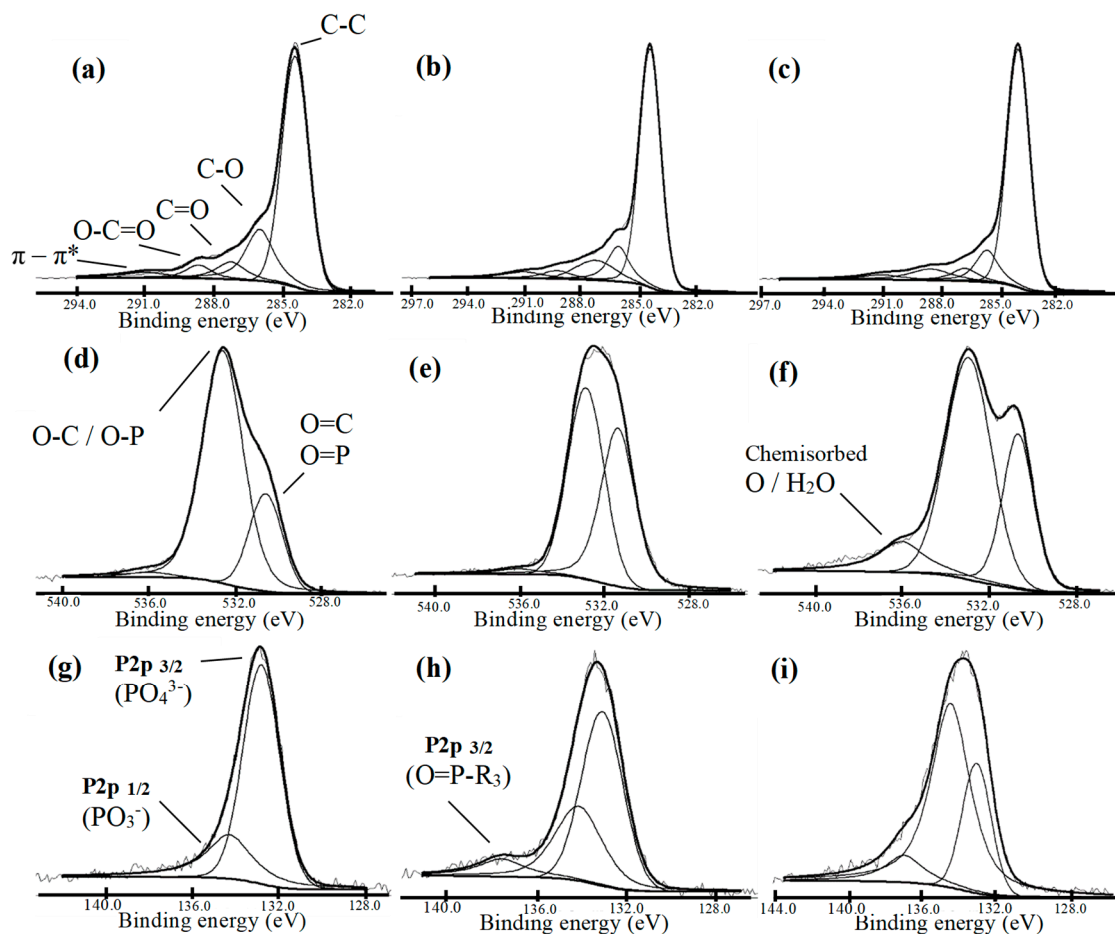


**Figure 2.** Representative examples of deconvoluted XPS spectra corresponding to the C1s (a–c), O1s (d–f) and P2p (g–i) regions of the following AC samples: (a) DA; (b) DL3A; (c) S300DA; (d) DL1A; (e) DFWA; (f) C2A; (g) DFA; (h) C6A; (i) S200CA.

For all AC samples there are two common contributions (Figure 2g–i), namely, P2p<sub>3/2</sub> and P2p<sub>1/2</sub>, which can be associated to isolated or linearly condensed phosphates, and to cyclic phosphates, respectively [29]. Considering the AC samples that are preceded by impregnation with diluted H<sub>3</sub>PO<sub>4</sub> solutions (including those performed on semi-carbonized CSs), the two mentioned contributions exhibit different relative abundances. The P2p<sub>3/2</sub> contribution at ~133.0 eV is far larger (nearly five times higher) than the P2p<sub>1/2</sub> one in most of the cases, indicating that the main phosphorus species on these ACs' surfaces are phosphates [31], again in good agreement with the FTIR spectra. The P2p<sub>1/2</sub> contribution at ~134.3 eV would correspond to cyclic phosphates such as metaphosphates (empirical formula PO<sup>3-</sup>), but not to neutral cyclic phosphorus oxides (for instance, P<sub>2</sub>O<sub>5</sub> species should appear at 136.5 eV [31]). When concentrated H<sub>3</sub>PO<sub>4</sub> solutions are used during the impregnation stage, the P2p<sub>1/2</sub> contribution gains greater significance as the abundance of metaphosphates is higher in these cases, even more than phosphates in particular cases (see sample S200CA, Figure 2i). Moreover, the phosphorus-based surface chemistry shows a new contribution at ~137.5 eV, which the literature sources ascribe to phosphazene and phosphine groups [32]. The presence of phosphazene can be discarded, as observed from the atomic surface composition (Table 1), where the nitrogen content in surface was negligible for the Series 2 samples, and also due to the lack of intense IR characteristic bands at ~790 (PNP bending), ~1200 and ~1250 (P=N stretchings) cm<sup>-1</sup> [33]. The most plausible explanation for this contribution would be the presence of phosphine oxide (O=P-R<sub>3</sub>), which would additionally contribute to the high intensity in FTIR bands at ~1180 cm<sup>-1</sup> (Figure 1b). This contribution shifts to lower binding energies (around a 0.5 eV

downshift) in AC samples with semi-carbonized feedstocks (samples S200CA and S300CA, see Figure 2i), suggesting a slightly different composition of these groups spawned by the CSs' thermal treatments before impregnation. Nonetheless, to the best of our knowledge, these chemical functionalities were only reported once, very recently, as functional groups in the surface of ACs made by  $\text{H}_3\text{PO}_4$  activation [34], but for the first time they have herein been confirmed by XPS.

#### 4. Conclusions

The spectroscopic and elemental characterization of different ACs produced from CSs and  $\text{H}_3\text{PO}_4$  reveals that the impregnation method is particularly influential on their resulting surface chemistry, meaning that the chemical nature of the ACs is sensitive to the preparation conditions. The hydrophilicity of ACs (on the basis of oxygen and moisture contents) depends on the  $\text{H}_3\text{PO}_4$  concentration and the semi-carbonization or not of the feedstock. Higher  $\text{H}_3\text{PO}_4$  concentrations and semi-carbonized CSs provide ACs with a more hydrophilic character and higher intensity in the phosphorus-related IR bands. The intensity and resolution of the ether and carbonyl bands is proportional to the  $\text{H}_3\text{PO}_4$  concentration employed during the impregnation step. The feedstock semi-carbonization at 300 °C leads to the appearance of phenol and carboxylic acid bands in the IR spectrum. The observations in FTIR spectra are perfectly compatible with the XPS characterization. XPS spectra showed that AC samples which were preceded by impregnation with diluted  $\text{H}_3\text{PO}_4$  solutions possessed a surface chemistry based on single-bonded C-O groups and linear phosphates, while those impregnated with concentrated  $\text{H}_3\text{PO}_4$  exhibited significantly higher amounts of C=O bonds, together with larger amounts of cyclic phosphates and the appearance of phosphine oxide functional groups, herein confirmed for the first time in ACs with the XPS technique. This present study reveals that the actuation over experimental procedure during the impregnation allows for control not only of the ACs' texture and porosity development, but also allows for the tuning of the surface chemistry of the resulting materials.

**Supplementary Materials:** The following supporting information can be downloaded at: <https://www.mdpi.com/article/10.3390/pr12010149/s1>, Figure S1: Graphical scheme depicting the samples preparation sequence (regarding the different impregnation methodologies with  $\text{H}_3\text{PO}_4$ ). Cherry stones are impregnated either with diluted (D)  $\text{H}_3\text{PO}_4$ , of 16 g/100 mL concentration, in single or multiple (DL, DI) impregnation steps adding up a total concentration equal to D, by filtration (DF) and/or washing (DFW), and using the residual liquid as the impregnation solution (DLR); or commercial concentrated (C)  $\text{H}_3\text{PO}_4$  of 144 g/100 mL concentration and their overconcentrated derived solutions by mildly heating it at different time in hours (C2, C4, etc.). The semi-carbonized cherry stones were also impregnated with either D or C  $\text{H}_3\text{PO}_4$  solutions. All impregnated samples ended up in activated carbon samples after heat treatment at 500 °C for 2h under a  $\text{N}_2$  atmosphere. Thus, the eventual sample name would end in -A.

**Author Contributions:** Conceptualization, J.M.G.-D. and V.G.-S.; methodology, V.G.-S., M.A.-F. and C.F.-G.; software, J.M.G.-D.; validation, V.G.-S.; formal analysis, J.M.G.-D.; investigation, J.M.G.-D.; resources, J.M.G.-D., M.A.-F. and V.G.-S.; data curation, J.M.G.-D.; writing—original draft preparation, J.M.G.-D.; writing—review and editing, J.M.G.-D., C.F.-G., M.A.-F. and V.G.-S.; supervision, V.G.-S. All authors have read and agreed to the published version of the manuscript.

**Funding:** This research received no external funding.

**Data Availability Statement:** Data is contained within the article and Supplementary Material.

**Conflicts of Interest:** The authors declare no conflict of interest.

#### References

1. Danish, M.; Ahmad, T. A Review on Utilization of Wood Biomass as a Sustainable Precursor for Activated Carbon Production and Application. *Renew. Sustain. Energy Rev.* **2018**, *87*, 1–21. [[CrossRef](#)]

2. Devi, R.; Kumar, V.; Kumar, S.; Bulla, M.; Jatrana, A.; Rani, R.; Mishra, A.K.; Singh, P. Recent Advancement in Biomass-Derived Activated Carbon for Waste Water Treatment, Energy Storage, and Gas Purification: A Review. *J. Mater. Sci.* **2023**, *58*, 12119–12142. [[CrossRef](#)]
3. Álvarez-Gutiérrez, N.; Gil, M.V.; Rubiera, F.; Pevida, C. Kinetics of CO<sub>2</sub> Adsorption on Cherry Stone-Based Carbons in CO<sub>2</sub>/CH<sub>4</sub> Separations. *Chem. Eng. J.* **2017**, *307*, 249–257. [[CrossRef](#)]
4. Venegas-Gómez, A.; Gómez-Corzo, M.; Macías-García, A.; Carrasco-Amador, J.P. Charcoal Obtained from Cherry Stones in Different Carbonization Atmospheres. *J. Environ. Chem. Eng.* **2020**, *8*, 103561. [[CrossRef](#)]
5. Malovanyy, M.; Bordun, I.; Ableeva, I.; Krusir, H.; Sahdeeva, O. *Synthesis of Activated Carbon from Plant Raw Materials by a Self-Activation Modified Method*; Trans Tech Publications Ltd.: Stafa-Zurich, Switzerland, 2021; Volume 1038, ISBN 9783035738896.
6. El-Nemr, M.A.; Hassaan, M.A.; Ashour, I. Formation of Self-Nitrogen-Doping Activated Carbon from Fish/Sawdust/ZnCl<sub>2</sub> by Hydrothermal and Pyrolysis for Toxic Chromium Adsorption from Wastewater. *Sci. Rep.* **2023**, *13*, 11556. [[CrossRef](#)] [[PubMed](#)]
7. Cunha, M.R.; Lima, E.C.; Lima, D.R.; da Silva, R.S.; Thue, P.S.; Seliem, M.K.; Sher, F.; dos Reis, G.S.; Larsson, S.H. Removal of Captopril Pharmaceutical from Synthetic Pharmaceutical-Industry Wastewaters: Use of Activated Carbon Derived from Butia Catarinensis. *J. Environ. Chem. Eng.* **2020**, *8*, 104506. [[CrossRef](#)]
8. Mani, D.; Elango, D.; Priyadharsan, A.; Al-Humaid, L.A.; Al-Dahmash, N.D.; Ragupathy, S.; Jayanthi, P.; Ahn, Y.-H. Groundnut Shell Chemically Treated with KOH to Prepare Inexpensive Activated Carbon: Methylene Blue Adsorption and Equilibrium Isotherm Studies. *Environ. Res.* **2023**, *231*, 116026. [[CrossRef](#)]
9. Lopa, N.S.; Bhadra, B.N.; Khan, N.A.; Zhuiykov, S.; Rahman, M.M. KOH/NaOH-Activated Carbon. In *Biomass-Based Supercapacitors: Design, Fabrication and Sustainability*; Wiley: Hoboken, NJ, USA, 2023; pp. 161–178. ISBN 9781119866435.
10. Ibrahim, M.; Souleiman, M.; Salloum, A. Methylene Blue Dye Adsorption onto Activated Carbon Developed from Calicotome Villosa via H<sub>3</sub>PO<sub>4</sub> Activation. *Biomass Convers. Biorefin.* **2023**, *13*, 12763–12776. [[CrossRef](#)]
11. Ahmed, T.A.; Abdulhameed, A.S.; Ibrahim, S.; AlOthman, Z.A.; Wilson, L.D.; Jawad, A.H. High Surface Area Mesoporous Activated Carbon Produced from Iraqi Reed via Pyrolysis Assisted H<sub>3</sub>PO<sub>4</sub> Activation: Box-Behnken Design for Surfactant Removal. *Diam. Relat. Mater.* **2023**, *133*, 109756. [[CrossRef](#)]
12. Liu, W.; Wang, X.; Zhang, M. Preparation of Highly Mesoporous Wood-Derived Activated Carbon Fiber and the Mechanism of Its Porosity Development. *Holzforschung* **2017**, *71*, 363–371. [[CrossRef](#)]
13. Zhang, J.; Yang, H.; Huang, Z.; Zhang, H.H.; Lu, X.; Yan, J.; Cen, K.; Bo, Z. Pore-structure regulation and heteroatom doping of activated carbon for supercapacitors with excellent rate performance and power density. *Waste Dispos. Sustain. Energy* **2023**, *5*, 417–426. [[CrossRef](#)]
14. Mehdi, E.; El, A.; Ojala, S.; Brahmi, R. Thermal treatment of H<sub>3</sub>PO<sub>4</sub>-impregnated hydrochar under controlled oxygen flows for producing materials with tunable properties and enhanced diclofenac adsorption. *Sustain. Chem. Pharm.* **2023**, *34*, 101164. [[CrossRef](#)]
15. González-Domínguez, J.M.; Fernández-González, C.; Alexandre-Franco, M.; Ansón-Casaos, A.; Gómez-Serrano, V. The Influence of the Impregnation Method on Yield of Activated Carbon Produced by H<sub>3</sub>PO<sub>4</sub> Activation. *Mater. Lett.* **2011**, *65*, 1423–1426. [[CrossRef](#)]
16. González-Domínguez, J.M.; Alexandre-Franco, M.; Fernández-González, C.; Ansón-Casaos, A.; Gómez-Serrano, V. Activated Carbon from Cherry Stones by Chemical Activation: Influence of the Impregnation Method on Porous Structure. *J. Wood Chem. Technol.* **2017**, *37*, 148–162. [[CrossRef](#)]
17. González-Domínguez, J.M.; Fernández-González, M.C.; Alexandre-Franco, M.; Gómez-Serrano, V. How Does Phosphoric Acid Interact with Cherry Stones? A Discussion on Overlooked Aspects of Chemical Activation. *Wood Sci. Technol.* **2018**, *52*, 1645–1669. [[CrossRef](#)]
18. Anisuzzaman, S.M.; Joseph, C.G.; Daud, W.M.A.B.W.; Krishnaiah, D.; Yee, H.S. Preparation and Characterization of Activated Carbon from Typha Orientalis Leaves. *Int. J. Ind. Chem.* **2015**, *6*, 9–21. [[CrossRef](#)]
19. Ruz, P.; Banerjee, S.; Das, T.; Kumar, A.; Sudarsan, V.; Patra, A.K.; Sastry, P.U. Tuning the Textural Properties and Surface Chemistry of Table Sugar Derived Activated Porous Carbons for Improved Hydrogen Storage. *J. Porous Mater.* **2023**. [[CrossRef](#)]
20. Azeez, M.O.; Tanimu, A.; Alhooshani, K.; Ganiyu, S.A. Synergistic Effect of Nitrogen and Molybdenum on Activated Carbon Matrix for Selective Adsorptive Desulfurization: Insights into Surface Chemistry Modification. *Arab. J. Chem.* **2022**, *15*, 103454. [[CrossRef](#)]
21. Valdés-Rodríguez, E.M.; Mendoza-Castillo, D.I.; Reynel-Ávila, H.E.; Aguayo-Villarreal, I.A.; Bonilla-Petriciolet, A. Activated Carbon Manufacturing via Alternative Mexican Lignocellulosic Biomass and Their Application in Water Treatment: Preparation Conditions, Surface Chemistry Analysis and Heavy Metal Adsorption Properties. *Chem. Eng. Res. Des.* **2022**, *187*, 9–26. [[CrossRef](#)]
22. Smith, M.; Scudiero, L.; Espinal, J.; McEwen, J.S.; Garcia-Perez, M. Improving the Deconvolution and Interpretation of XPS Spectra from Chars by Ab Initio Calculations. *Carbon* **2016**, *110*, 155–171. [[CrossRef](#)]
23. Bryś, A.; Zielińska, J.; Głowacki, S.; Tulej, W.; Bryś, J. Analysis of Possibilities of Using Biomass from Cherry and Morello Cherry Stones for Energy Purposes. *Proc. E3S Web Conf.* **2020**, *154*, 01005. [[CrossRef](#)]
24. Barkauskas, J.; Tautkus, S.; Kareiva, A. Residual Content of Inorganic Ions in Activated Carbons Prepared from Wood. *J. Anal. Appl. Pyrolysis* **2004**, *71*, 201–212. [[CrossRef](#)]
25. Romanos, J.; Beckner, M.; Stalla, D.; Tekeei, A.; Suppes, G.; Jalisatgi, S.; Lee, M.; Hawthorne, F.; Robertson, J.D.; Firlej, L.; et al. Infrared study of boron—Carbon chemical bonds in boron-doped activated carbon. *Carbon* **2013**, *54*, 208–214. [[CrossRef](#)]

26. Coates, J. Interpretation of Infrared Spectra, a practical approach. In *Encyclopedia of Analytical Chemistry*; Meyers, R.A., Ed.; John Wiley & sons Ltd.: Chichester, UK, 2000; pp. 10815–10837.
27. Puziy, A.M.; Poddubnaya, O.I.; Martínez-Alonso, A.; Castro-Muñiz, A.; Suárez-García, F.; Tascón, J.M.D. Oxygen and phosphorus enriched carbons from lignocellulosic material. *Carbon* **2007**, *45*, 1941–1950. [[CrossRef](#)]
28. Figueiredo, J.L.; Pereira, M.F.R.; Freitas, M.M.A.; Orfao, J.J.M. Modification of the Surface Chemistry of Activated Carbons. *Carbon* **1999**, *37*, 1379–1389. [[CrossRef](#)]
29. Puziy, A.M.; Poddubnaya, O.I.; Socha, R.P.; Gurgul, J.; Wisniewski, M. XPS and NMR Studies of Phosphoric Acid Activated Carbons. *Carbon* **2008**, *46*, 2113–2123. [[CrossRef](#)]
30. Figueiredo, J.L.; Pereira, M.F.R. The Role of Surface Chemistry in Catalysis with Carbons. *Catal. Today* **2010**, *150*, 2–7. [[CrossRef](#)]
31. Puziy, A.M.; Poddubnaya, O.I.; Ziatdinov, A.M. On the Chemical Structure of Phosphorus Compounds in Phosphoric Acid-Activated Carbon. *Appl. Surf. Sci.* **2006**, *252*, 8036–8038. [[CrossRef](#)]
32. Wagner, C.D.; Riggs, W.M.; Davis, L.E.; Moulder, J.F.; Mullenberg, G.E. *Handbook of X-ray Photoelectron Spectroscopy*; Perkin-Elmer Corp.: Eden Prairie, MN, USA, 1979.
33. Carriedo, G.A.; García Alonso, F.J.; González, P.A.; Menéndez, J.R. Infrared and Raman Spectra of the Phosphazene High Polymer  $[\text{NP}(\text{O}_2\text{C}_{12}\text{H}_8)]_n$ . *J. Raman Spectrosc.* **1998**, *29*, 327–330. [[CrossRef](#)]
34. Preglo, A.R.; Namata, J.; Caculba, J.; Sanchez, G.; Joyno, C.; Pagalan, E.; Arazo, R.O. Paracetamol Removal from Aqueous Solution through Activated Carbon from Mango Seeds. *Chem. Afr.* **2023**, *6*, 699–710. [[CrossRef](#)]

**Disclaimer/Publisher’s Note:** The statements, opinions and data contained in all publications are solely those of the individual author(s) and contributor(s) and not of MDPI and/or the editor(s). MDPI and/or the editor(s) disclaim responsibility for any injury to people or property resulting from any ideas, methods, instructions or products referred to in the content.